

1 Muon track reconstruction and veto performance 2 with D-Egg sensor for IceCube-Gen2

The IceCube Gen2 Collaboration

http://icecube.wisc.edu/collaboration/authors/icrc17_gen2

E-mail: achim.stoessl@icecube.wisc.edu

The planned extension of IceCube, IceCube-Gen2, a cubic-kilometer sized neutrino observatory, aims at increasing the rate of observed astrophysical neutrinos by up to a factor of 10. The discovery of a high energy neutrino point source is one of its primary science goals. Improving the sensitivity of the individual modules is a necessity to achieve the desired design goal of IceCube-Gen2. A way of improving their sensitivity is the increase of photocathode area. The proposed module called the D-Egg will utilize two 8" Hamamatsu R5912-100 photomultiplier tubes (PMTs), with one facing upwards and one downwards. These PMTs have an increased quantum efficiency and their sensitivity is comparable to the 10" PMT used by IceCube. This essentially leads to an increase in sensitivity by almost a factor of 2 with a full 4π solid angle acceptance. A simulation study is presented that indicates improvement in angular resolution using current muon reconstruction techniques due to the new sensor design. Since the proposed module is equipped with an upward facing PMT, further emphasis will be set on the development of new reconstruction techniques that exploit this geometry, as well as an improvement of veto probability for incoming muon tracks, which is crucial for neutrino astronomy in the Southern sky.

Corresponding author: A. Stoessl^{*1}

¹*International Center for Hadron Astrophysics, Graduate School of Science, Chiba University 1-33, Yayoi-cho, Inage-ku, Chiba-shi, Chiba, 263-8522 JAPAN*

*35th International Cosmic Ray Conference – ICRC2017-
10-20 July, 2017
Bexco, Busan, Korea*

*Speaker.

3 **1. IceCube Gen2**

4 The neutrino observatory IceCube at the geographic South Pole is a cubic kilometer array of
 5 photosensors which is able to detect the faint Cherenkov light produced by secondaries from inter-
 6 actions of neutrinos with the glacial ice[1]. So far, the experiment has yielded a plethora of science
 7 results, among them the discovery of a neutrino flux most likely of extraterrestrial origin[3]. After
 8 6 years of data-taking, with the completed detector, a precise measurement of the extraterrestrial
 9 neutrino flux is still limited by statistics. To overcome the statistical limitations and to improve the
 10 effective area for neutrino events in the energy regime beyond 10 PeV as well as the point source
 11 sensitivity, an extension of the IceCube array has been proposed[4]. The proposed geometry for
 12 IceCube-Gen2 considered in this work is shown in figure 1. The geometry shows a larger exten-
 13 sion in the x-y plane than in depth. It is optimized for the reconstruction of horizontal muon tracks,
 since these have the highest contribution to the point-source sensitivity[5].

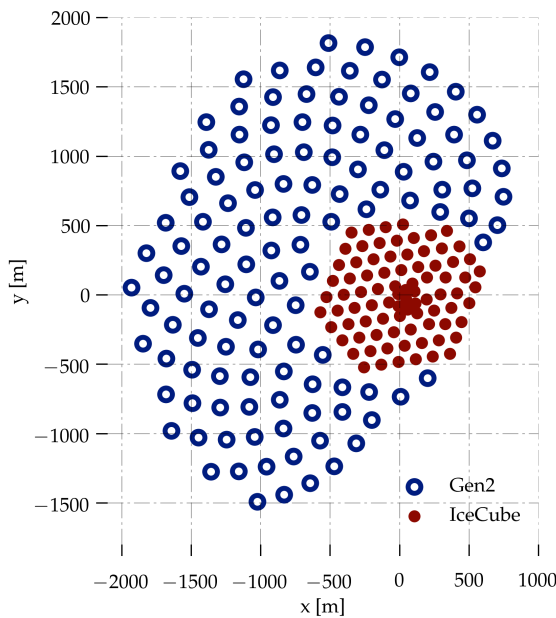


Figure 1: A proposed geometry for IceCube-Gen2 which is used for this study. In addition to the 86 strings of IceCube, which can be seen as the hexagonal shape marked with the red dots, 120 new strings with each 80 sensors are arranged in a complex grid geometry to optimize the veto power for incoming muon tracks. The extension of IceCube to larger positive x-values is prohibited due to the runway of the South Pole Station.

14
 15 **2. The D-Egg sensor for Gen2**

16 Several different sensor designs for IceCube-Gen2 are under investigation, however relevant
 17 for this study are the following two proposed designs:

- 18 ▶ The PDOM[7], which is basically the same design as the IceCube optical sensor[6], however
 19 with a PMT with a higher quantum efficiency. It features a single 10“ PMT which is facing
 20 downwards and a improved readout.
- 21 ▶ The D-Egg[8], which follows the design of the PDOM, however includes another PMT fac-
 22 ing upwards. The PMTs are 8“, so the total diameter of the D-Egg is slightly smaller than
 23 the PDOM and it has about 1.48 more photocathode area than the PDOM for a Cherenkov
 24 weighted spectrum.

25 A third design is worth mentioning in this context[9], since it exploits the idea of multiple sensors
 26 even further. Due to high drill costs at the South Pole, it is desirable to deploy sensors with a
 27 large photocathode area to keep the cost for the average cm^2 photocathode as low as possible. The
 28 high drill costs can be reduced by drilling holes with a smaller diameter, and thus as the diameter
 29 of the D-Egg is 10% smaller than the diameter of the PDOM, about 20% of the fuel cost can be
 30 saved during deployment. A graphic of the D-Egg with its dimensions is shown in figure 2. The
 31 two Hammaatsu R5912-100 high quantum efficiency PMTs are enclosed in a highly transparent
 32 glass housing, which is optimized for transparency in the near ultraviolet. The high voltage for the
 33 PMTs is generated on two boards, and the final design will feature a board for readout electronics
 34 as well. In this proceeding, we investigate the performance of the D-Egg using several existing
 35 reconstruction methods developed for IceCube and compare the results against the benchmark
 PDOM performance.

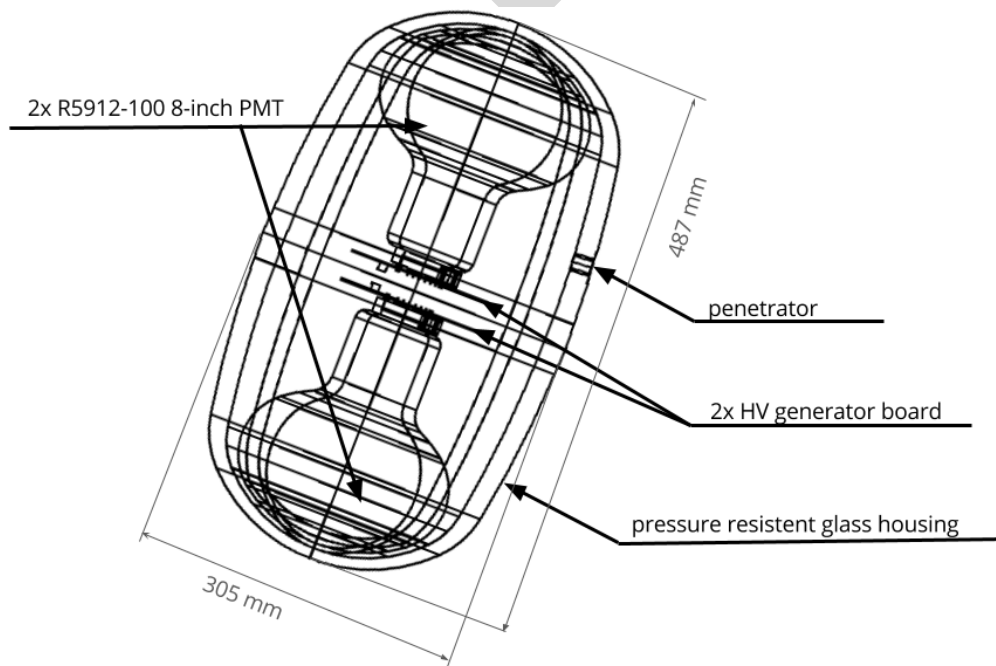


Figure 2: A schematic of the D-Egg design. It features two 8" PMTs enclosed in a highly transparent glass housing. Its diameter is 10% smaller than that of the current IceCube optical module.

36

37 3. Simulation

38 We simulated muons from an $E^{-1.4}$ power-law spectrum in the energy range of 10 TeV to 10
 39 PeV with a full 4π angular distribution. The muons were injected at a cylindrical surface enclosing
 40 the detector and then propagated through the ice. The light emerging by stochastic energy losses
 41 of the muons as well as the smooth Cherenkov light were simulated and the photon propagation is
 42 handled by the software clsim[]. The simulation features a bulk ice model which means that the ice
 43 is homogenous throughout the detector. As the direct propagation is time consumptive, the detector
 44 simulation for D-Egg and PDOM are sharing the same photon simulation as input. To further

45 increase the simulation efficiency, several simplifications were made. Consequently, the effects
 46 of glass and gel and the module geometry are not simulated individually, instead the photons are
 47 weighted with the angular sensitivity of the module as well as the wavelength dependent quantum
 48 efficiency. The efficiency of the photocathode is assumed to be constant over the whole area. To
 49 further increase the efficiency of the simulation, the size of the modules is scaled up and the number
 50 of propagated photons is decreased accordingly.
 51 The noise introduced by the PMT and the glass housing is simulated in the same way for D-Egg
 52 and PDOM, however with absolute values scaled by the photocathode area. Further simplifications
 53 are made in the PMT and sensor simulation. The PMT simulation is done as for the PMT used in
 54 IceCube, as they are very similar in their behavior. The benefit of this is that the same simulation
 55 chain can be used for D-Egg as well as for the IceCube DOM and PDOM. As the readout electronics
 56 for the D-Egg is not yet finalized, we assume a perfect readout with an infinitesimal small binning
 in time. The IceCube array, as part of IceCube-Gen2 has been simulated to our best knowledge.

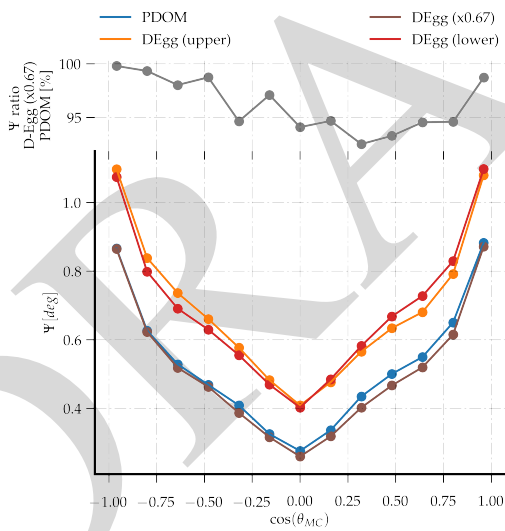


Figure 3: The results of the SPEFit reconstruction for both sensors, D-Egg and PDOM binned in the cosine of the simulated muon direction. The D-Egg effective area is scaled down by a factor of 0.67 to match the PDOM effective area. Muons with a cosine of -1 are entering the detector from below, those with 1 from above respectively.

57

58 4. Muon reconstruction

59 The simulated dataset was reconstructed with a set of algorithms. In this study we focus on the
 60 reconstruction algorithms SPEFIT and SPLINE-RECO[1]. The algorithms operate on the recon-
 61 structed pulses, each using a different method. While SPEFIT uses a simple analytical ice-model
 62 and a likelihood with one term per optical module, where only the first registered pulse is consid-
 63 ered, SPLINE-RECO is capable of constructing a likelihood with a pdf obtained from tabulated
 64 values, and thus is able to also include more complicated models for the glacial ice. To compare
 65 the accuracy of the reconstruction results, we looked at the distributions of the opening angle Ψ
 66 between the simulated and reconstructed track. The median of this distribution is used as a figure
 67 of merit. No quality cuts have been applied, yet we restrict ourself to tracks which traverse the
 68 instrumented volume.

69 We aim to investigate the impact of the increased photocathode area and segmentation on the re-
 70 construction independently. As such, we work with different types of D-Egg simulation:

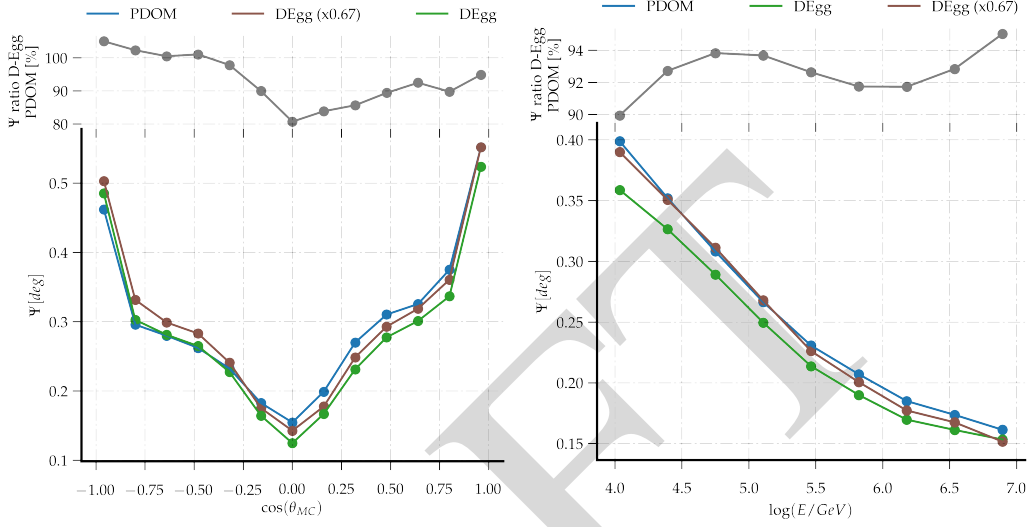


Figure 4: The results of the reconstruction SPLINE-RECO, binned in the cosine of the simulated muon direction on the left and binned in the logarithm of the muon energy on the right. Muons with a cosine of -1 are entering the detector from below, those with 1 from above respectively.

- 71 ▶ Simulation of the D-Egg “as is” as described in section 3.
- 72 ▶ The same as above, however the effective photocathode area is scaled down by a factor of
- 73 0.67 to match the photocathode area of the PDOM
- 74 ▶ Simulation of the D-Egg where either the upward or downward facing PMT is disabled.

75 All types of simulations share the same simulated photons, but then branch in different detector
 76 simulations. First, the behavior of the two individual PMTs is studied. As the simulation has up-
 77 down symmetry, we expect the same performance for the datasets with only pulses in the upper or
 78 lower PMT. The results for the SPEFIT reconstructions is shown in figure 3. All reconstructions
 79 perform best for more horizontal events due to the fact that the Gen2 geometry, as shown in figure
 80 1, is elongated more in the x and y dimension than in the z dimension. This means that horizontal
 81 tracks cross a larger instrumented volume. Also as the string spacing is 240 m, vertical tracks have a
 82 lower light yield if they enter the detector in between strings. For up going muons, if only the lower
 83 PMT of D-Egg is used as reconstruction input, it can be seen that the performance is slightly better
 84 than for the upper PMT only, and vice versa for down-going muons. The SPEFIT reconstruction
 85 yields a higher accuracy for the D-Egg sensor, which we quantify to be about 5% in the horizontal
 86 and downward region due to the segmentation of the D-Egg only as we here compare to the scaled-
 87 down version. We attribute this to the fact that SPEFit uses only the first pulse recorded by each
 88 PMT, and the doubling of PMT thus increases the number of pulses available to the reconstruction,
 89 especially for the downward region.

90 The performance SPLINE-RECO of the reconstruction is shown in figure 4. The D-Egg exhibits
 91 up to 15% higher accuracy in reconstruction especially in the horizontal region, which is important
 92 to point source searches[]. The reconstruction in the down-going region yields more accurate
 93 results with D-Egg as well. Comparing the results as a function of the true muon energy E_{MC} , the

94 SPLINE-RECO reconstruction gains due to the higher photoelectron yield, which is shown for
 95 the two sensor modules in figure 4. However it seems that most of the gain results from the larger
 96 photocathode area of D-Egg.

97 5. Likelihood improvements for segmented sensors

98 Figure 4 shows that the increase in reconstruction performance for the D-Egg seems to be
 99 attributed mostly to its larger total photocathode area. Thus, we investigate the details of the
 100 SPLINE-RECO reconstruction, which is developed for IceCube and not optimized for segmented
 101 sensors, and thus it may not exploit the full potential of highly segmented detector configuration.
 102 Developed for IceCube, the here used likelihood is not optimized for segmented sensors, and thus
 103 it does not exploit their full potential. The likelihood is given by:

$$L = \prod_{j=1}^{N_{DOM}} N \cdot p_j(t_j) \cdot (1 - P_j(t_1))^{N-1} \quad (5.1)$$

104 In the above equation, N stands for the number of hits on a certain optical module, p_j and P_j are
 105 the time residual pdf and cdf for the hit DOM and t_j is the time of the first hit of the given DOM.
 106 Contours of this likelihood function can be seen in figure 5. This simplified example illustrates
 107 the likelihood space for a single module, placed in the middle of the individual figures. A muon
 108 track crosses the plane of the figure orthogonal in 120 m distance with an expectation of 20 pho-
 109 toelectrons, and 1σ likelihood contours are indicated. The likelihood developed for the IceCube
 110 DOM is shown with the red color. As it can be seen, it is rather agnostic to the direction of the
 111 individual PMT and imposes only very small constraints on the likelihood contour. As a reason,
 112 we suspect the importance of the late photons in the arrival time distribution, which are not well
 113 considered in the current approach, as it focuses on the unscattered photons from the Cherenkov
 114 cone of the track. However if their timing is considered, these late, scattered photons can contribute
 115 significantly to constraining the likelihood. Extending equation 5.1 and rewriting it including the
 116 arrival times of late photons can improve the likelihood, as it is illustrated in the example. The
 117 IceCube-Gen2 collaboration is currently working on a reconstruction implementing this approach,
 118 yet it is not production ready at the time of this work.

120 6. Veto performance

121 An effective method to select an all flavor neutrino sample with high purity and full sky accep-
 122 tance is the implementation of a veto: Using the outer strings and top and bottom layer of optical
 123 modules, incoming muon tracks can be tagged and removed from such a sample. The method has
 124 been proven successful and lead to the discovery of the extraterrestrial neutrino flux[3].
 125 The method has been applied and studied for IceCube-Gen2[11]. In the context of this proceedings
 126 we are investigating the impact of D-Egg on the efficiency of the veto algorithm. An important
 127 parameter of the current algorithm is the veto threshold, which is the charge required in the veto
 128 region to trigger the veto, which is currently set to 3 PE. Since the D-Egg has an upward facing
 129 PMT, we expect a higher performance for down-going cosmic ray muon tracks. Due to the D-Eggs

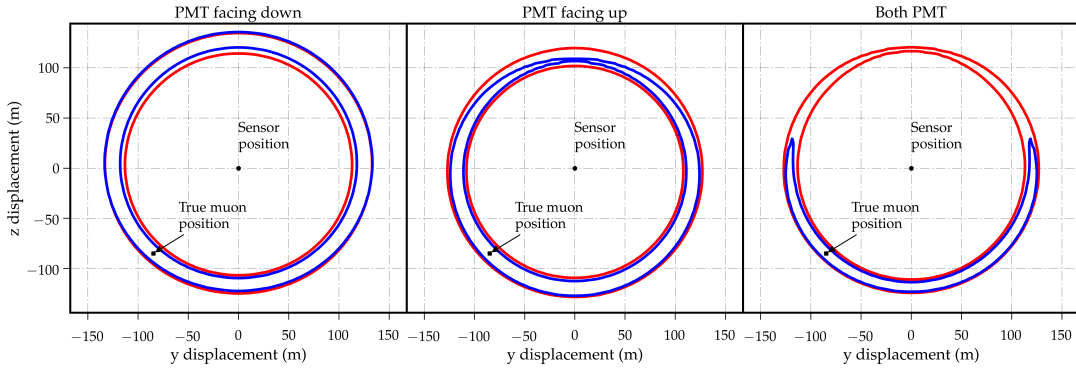


Figure 5: Likelihood contours of two different likelihoods for a single D-Egg sensor in case of a muon traversing the plane in orthogonal direction. The red contour results from the likelihood used in SPLINE-RECO, the blue contour is a proposed likelihood considering the timing of the late pulses in the arrival time distribution. On the left, the contours are shown for the lower PMT only. The contours are based on an Asimov test. The middle plot shows the situation for the upper PMT and on the right the combined contours of both PMTs are shown.

130 larger photo cathode, we also expect a higher probability to detect charge in the veto region at all.
 131 This is illustrated in figure 6: The distribution of collected charge for the upper 2 layers of modules
 132 of the IceCube-Gen2 sunflower geometry is significantly shifted for the use of D-Eggs to lower
 133 values, which results in a higher probability to veto incoming muons. Further impact of the use of
 D-Eggs in the veto region is currently under investigation.

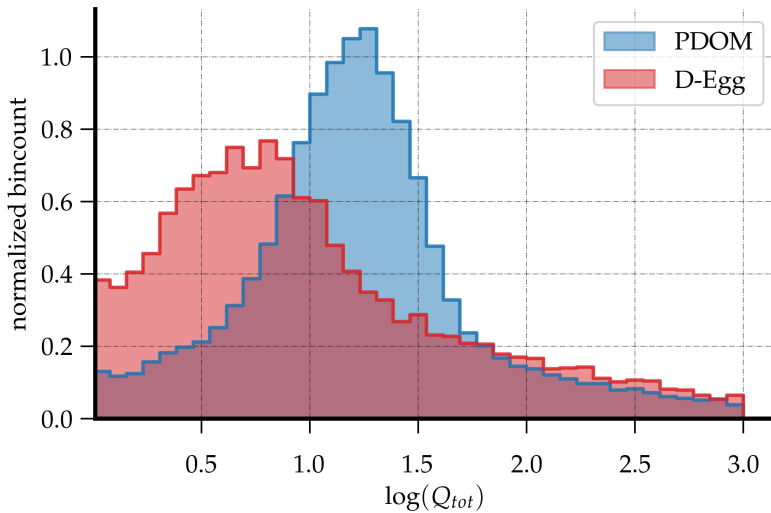


Figure 6: The collected charge in the upper layer of the IceCube-Gen2 array. The collected charge is shown for the uppermost 2 layers of optical modules. In the case of D-Egg, a much higher contribution in the onset region around 3 PE has been found.

134

135 7. Summary

136 For the first time, we present a study of muon track angular resolutions with current
 137 reconstruction techniques used by IceCube. We compare a new sensor design, the D-Egg, to an
 138 improved sensor based on the current IceCube design (PDOM). Despite with the advantage of
 139 higher segmentation, the performance of the D-Egg is increased by no more than 20% for the

140 angular resolution in comparison with the PDOM. We attribute most of this increase to the
141 increased photocathode area, which is increased by 48% compared to the PDOM.
142 By studying why the higher segmentation only gives minor impact on reconstruction, we find the
143 reason in the likelihood of the SPLINE-RECO reconstruction: By not considering the timing of
144 the late pulses properly, the information in the late part of the arrival time distribution of the
145 photons in the individual sensors is lost. Including the timing information of the late pulses in the
146 likelihood we can improve the reconstruction in such a way, that it is able to identify the
147 directionality of a muon track with only a single sensor in the best-case scenario.
148 Besides the improvement in angular resolution, we show that the veto performance for the current
149 implementation of the IceCube veto can be improved by using D-Eggs as well. We studied the
150 deposited charge in the upper layer of the IceCube-Gen2 array and find a significant increase in
151 the low charge region around the 3 PE threshold. In conclusion, we find that we are on a good
152 track to improve the current IceCube reconstruction and veto techniques to exploit the full
153 potential of new approaches in sensor design for IceCube-Gen2 and encourage further, more
154 detailed studies to follow.

155 References

- 156 [1] **IceCube** Collaboration, A. Achterberg et. al., *APP* **26** (2006) P155-173.
157 [2] **IceCube** Collaboration, M.G. Aartsen et. al., *SCI* **342(6161)** (2006) P1242856.
158 [3] **IceCube** Collaboration, M.G. Aartsen et. al., *PRL* **131** (2014) P101101.
159 [4] **IceCube** Collaboration, M. G. Aartsen et al., *astro-ph/1412.5106* (2014).
160 [5] **IceCube-Gen2** Collaboration, *PoS (ICRC2017) 991* (these proceedings).
161 [6] K. Hanson and O. Tarasova, *NIM* **567(1)** (2006) P214-217
162 [7] **IceCube-PINGU** Collaboration, P. Sandstrom, *AIP* **1630(1)** (2014) P180-183.
163 [8] **IceCube-Gen2** Collaboration, *PoS (ICRC2017) 1051* (these proceedings).
164 [9] **IceCube-Gen2** Collaboration, *PoS (ICRC2017) 1047* (these proceedings).
165 [10] **AMANDA** Collaboration, J. Ahrens et al., *NIMA* **524** (2004) P169-194.
166 [11] **IceCube-Gen2** Collaboration, *PoS (ICRC2017) 945* (these proceedings).